Multiscale Modeling of Molecule Transport through Skin's Deeper Layers

Nitu Verma[1]*, Kishore Gajula[2]*, Rakesh Gupta[1§], Beena Rai[1]

1. TCS Research, Tata Research Development and Design Centre, Pune – 411013, India
2. TCS Research, Hyderabad - 500034, India.

(*equal contribution)

§ Corresponding author: gupta.rakesh2@tcs.com

Abstract

Accurate *in-silico* models of human skin are required to obtain the uptake/release of molecules across the skin layers to supplement the *in-vivo/in-vitro* experiments for faster development/testing of cosmetics and drugs. We aim to develop an *in-silico* skin permeation model by extending the multiscale modeling framework developed earlier for skin's top layer to deeper layer and compared the outcomes with *in-vitro* experimental permeation data of 43 cosmetic-relevant molecules across human skin.

In this study, we have extended a multiscale modeling framework, with realistic heterogeneous stratum corneum (SC) comprising of network of permeable lipids and corneocytes, followed by homogeneous viable epidermis and dermis. The diffusion coefficients of molecules in lipid layer were determined using molecular dynamics simulations, whereas the diffusion coefficients in other layers and all the partition coefficients were calculated from correlations reported in literature. These parameters were then used in the macroscopic models to predict the release profiles of drugs through the deeper skin layers. The obtained release profiles were in good agreement with available experimental data for most of the molecules. The reported model could provide insight into cosmetics/drugs skin permeation and act as a time-saving and efficient guiding tool for performing targeted experiments.

1 Introduction

Over the past decades, researchers have put significant efforts in understanding the human skin barrier and its functionalities and leveraging it for several personal and healthcare applications. Morphologically, the skin is the largest external organ with an area of approximately 1.7 m^2 providing a natural chemical and biological barrier [1, 2, 3]. The human skin mostly has three layers and accounts

for around 16% of the total body mass [1, 4] . These layers are arranged from the outer to the inner layers as follows: epidermis, dermis, and hypodermis or subcutaneous tissues [1, 5, 6]. The top layer of the epidermis, stratum corneum (SC), provides a chemical barrier by selectively allowing molecules with specific physical and chemical properties, dermis provides mechanical support to skin and hypodermis regulates the temperature of skin [7, 8]. Owing to its high surface area the skin is an attractive target for various topical and personal care applications, but presence of SC barrier makes it challenging. The topical or transdermal drug delivery have advantages over traditional routes such as avoiding loss of active ingredient due metabolism in stomach in oral route, the pain and compliance issues related to injections to name a few [9]. Hence, around 40 % drugs under clinical assessment involve transdermal or dermal delivery [10].

The transport of molecules across the skin is a multistep process. a) transport of the molecules with in the delivery system, b) chemical partitioning of molecules into SC (either lipid matrix or corneocyte), c) diffusion and binding of the molecules inside the SC layer (including diffusion and partitioning between lipids and corneocytes layers), d) partitioning of the molecules from the SC layer into the VE layer, e) binding and diffusion of the molecules across the VE layer, f) partitioning of the molecules from the VE layer into dermis layer, g) binding and diffusion of the molecules across the dermis layer, h) elimination of the molecules from the dermis layer by blood capillaries [1, 11, 12, 13]. Thus, the transport process of molecules through the skin layers is profoundly intricate because each layer has its own biophysical or biochemical characteristics.

The products design either for drug delivery or cosmetic application involves transport of molecules across one or more layers of the skin. The development of these products requires in depth permeation studies which are usually conducted using detailed *in-vitro/in-vivo* experiments. The uprising of animal rights movements and global campaigning efforts culminated with the phasing out of animal testing in cosmetics within European Union (EU) [14]. In addition, the 7th Amendment to the Cosmetic Directive (Directive 76/768/EEC) and REACH demanded the development of novel *in vitro* methods for future risk assessment of chemicals for their potential to cause toxicity [15, 16]. In response to this, the Cosmetics Europe ADME Task Force (TF) launched several projects towards alternative testing methods and came up standardization protocol of *in-vitro* and *in-silico* studies [16, 17, 18]. Ellison et al. [16] developed a standard protocol to generate physiochemical (partition coefficient (K) and diffusion coefficient (D)) properties of 50 cosmetic relevant molecules for different skin layers. Hewitt et al. [17], developed OECD test guideline 428 compliant protocol using human skin to test the permeation of 56 cosmetic-relevant molecules using *in vitro* assays. While *in vitro* studies have proved to provide information on permeation on single application of molecules into skin, but long-term

exposure such as repeated use of cosmetics is difficult to study. The instability and sensitivity of some molecules may also pose difficulty in transdermal permeation study using *in vitro* assays. Various *in-silico* models have been investigated to address this gap. Grègoire et al. [18], investigated 3 open source (DermWin™, CDC and the University of Surrey models) and 3 commercial (DSkin, SimCyp and TCAT) *in silico* models for permeation of 25 cosmetic relevant compounds and compared their dermal delivery (DD: amount present in dermis, VE and receptor fluid (RF)) with those from in vitro study done by Hewitt et al. [17]. They reported correlation coefficient (r^2) for the various model under different physiochemical properties of molecules; TCAT(r^2 ~0.8), DSkin (r^2 ~0.6), SimCyp(r^2 ~0.57), CDC(r^2 ~0.58), Surrey(r^2 ~0.28). These in-silico models used different methods for obtaining the physiochemical properties (i) measured D and K from experimental *in vivo* studies [16] comprising of homogeneous SC, followed by VE and dermis, (ii) predicted D and K from various QSARs model consisting of heterogeneous SC with lipid and corneocytes layers, followed by VE and dermis. TCAT model gave the best result (r^2 ~0.8) when evaluated with predicted D and K but used adjusted initial dose based on experimental mass balance (MB) to account for chemical volatility without modifying the model dynamics. Similarly, SimCyp used adjusted initial dose for evaporation but gave better result (r^2 ~0.57) with measured D and K. The Surrey model based on Chen et al. [19] used nominal dose from Hewitt et al. [17] and measured D and K to get a poor correlation r^2 ~0.28. Here, the evaporation of molecules was incorporated into permeation dynamics, but the evaporative mass transfer coefficient was corrected based on MB. CDC based on spreadsheet-based model [20, 21, 22] used nominal dose and predicted D and K with evaporation of molecules based on chemical volatility and wind velocity incorporated into diffusion dynamics and resulted in r^2 ~0.58. DSkin model again gave r^2 ~0.6 when using predicted D and K with nominal dose and solute evaporation was considered. Thus, although these models have given good results, but this could further be improved by modifying few of the model features. A realistic *in-silico* multiscale model for deeper skin layers with heterogeneous SC and with chemical evaporation based on chemical volatility and external conditions (wind velocity, temperature) with accurate physiochemical properties could make the permeation dynamics more robust and further improve the correlation with experimental results.

There are a few more studies reported on the macroscopic modeling of skin [23, 24, 25, 26, 19, 21]. Rim et al. [23] presented a mathematical model for multicomponent nonlinear diffusion considering the coupling effects between the different components and used it for studying the diffusion from a finite drug reservoir patch into the skin using finite element method. Rim et al. [24] carried out a multiscale simulation with homogenized SC and VE for studying multicomponent transdermal drug delivery application. Kushner et al. [25] modelled the skin SC lipid pathway from first principles

approach to come up with the modified Fick's 2nd law to account for the existing branched pathways in the SC and developed the two-tortuosity model. Frasch et al. [26] presented two-dimensional Finite element model (FEM) model for diffusion through the SC brick and mortar lipid pathway. Steady-state flux and lag time of the heterogenous SC were found to be good agreement with that of homogeneous membrane of the same thickness consisting of lipid material. Chen et al. [19] developed a mechanistic mathematical model for predicting the pharmacokinetics of molecules permeating through the skin and into the blood circulation using finite difference method and validated using clinical data. Miller et al. [21] developed a spreadsheet-based method to analyze the simultaneous absorption and evaporation from a multicomponent formulation applied on to the skin. Diffusion here occurred through homogeneous SC and homogenous VE and dermis with identical transport parameters was considered and predicted significantly better absorption with the multicomponent vehicle model than with simpler models that track only one component.

Although many studies reported in literature for modeling molecule permeation through the skin, they are limited to individual layers of the skin and SC is assumed to be a homogeneous membrane [24, 26, 27, 28]. As discussed earlier, SC is not homogenous in nature and providing the main barrier for the transport across the skin. To bridge this gap, modeling molecule permeation across skin layers, accounting for heterogeneity of SC is necessary.

In this study, we have modified the *in-silico* skin model developed earlier [27] by integrating the atomistic/molecular level models of SC lipid matrix with the macroscopic model of the deeper layers of skin. The composition and configurations of individual layers of skin were obtained from earlier experimental studies [29, 30, 31]. The transport and thermodynamics properties of these layer depend upon the composition and hence appropriate compositions were chosen to accurately represent the barrier properties [32, 33, 34]. The SC is represented by its heterogeneous structure in brick-and-mortar fashion in which the corneocytes synonyms to brick are suspended in mortar of lipid matrix [35]. On the other hand, viable epidermis and dermis are modeled as homogenized material with properties related to the main compositions of cellular lipid, protein and water [36]. Based on properties and composition of these layers, various correlations for their physiochemical parameters have been reported in literature [19, 25, 37, 38, 22] which are used in this study.

We report an integrated multiscale modeling framework which would provide insight into the permeation mechanisms of the molecule through skin and investigated skin permeation of 43 cosmetic-relevant chemicals taken from Ellison et al. [16] and Hewitt et al. [17]. This work is an extension to our previous work on multiscale modeling of SC where infinite dosage conditions with non-permeable

corneocytes were considered [27]. In the current study finite dosage conditions are considered with permeable corneocytes along with other skin layers viable epidermis and dermis. The physical parameters such as diffusion coefficient and partition coefficients are either obtained using molecular dynamics (MD) simulations or empirical correlations from the literature. Further, the release profiles obtained using integrated multiscale models are compared with the existing literature [17].

2 Methods and Models

2.1 Molecular Simulation

The SC mainly made up of corneocytes (brick) and lipid matrix (mortar). A heterogeneous mixture of long chain ceramides (CER), cholesterol (CHOL) and free fatty acid (FFA) in certain ratios makes up the lipid matrix [39, 40]. To simulate a realistic SC layer [41], we have chosen the most abundant ceramide, CER-NS 24:0 and free fatty acid, FFA 24:0 for molecular model from our earlier studies [42]. The force field parameters for the CER were taken from the Berger et al and GROMOS87 parameters [43]. The charges on polar groups were taken from earlier simulation study [44, 45, 46]. The parameters for FFA and CHOL were taken from the Holtze et al. [47]. The molecules were modelled using Gromos 54a7 [48] force field. The simple point charge model was used for water molecules [49].

The simulations were carried out in NPT ensemble using the GROMACS molecular dynamics package [50, 51, 52, 53, 54]. Pressure was controlled by Parrinello-Rahman barostat and kept at 1 bar with compressibility of 4.5×10^{-5} bar and a time constant of 5 ps. The temperature was controlled at 310 K by Nose-Hoover thermostat with a time constant of 0.5 ps and the coupling was done separately to lipid molecules and water. All the bonds in lipid and permeate molecules were constrained using LINCS algorithm [55] while SETTLE algorithm was used for water. A cut off 1.2 nm was used for van-der Waals and electrostatic interactions. The systems were periodic in all three directions. Long range electrostatic interactions were computed using particle mesh Ewald (PME) method.

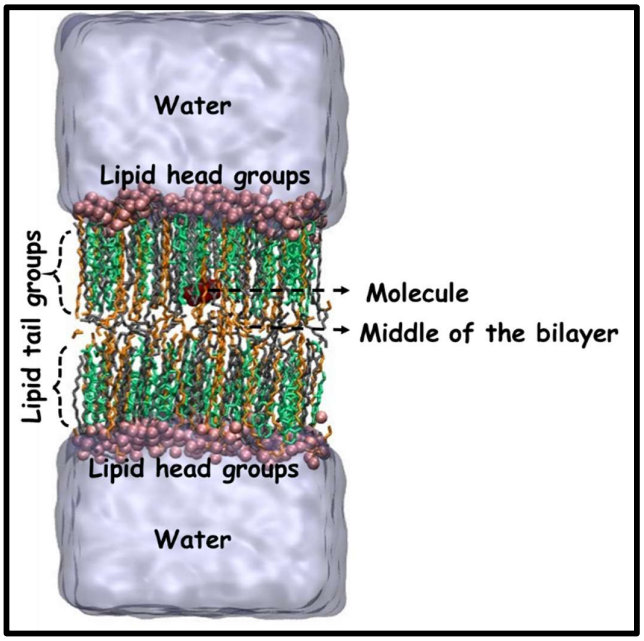

Figure 1: Side view of simulation snapshot of molecule constrained in the bilayer. The molecule was kept at a distance of ~ 1nm from COM of bilayer. Images were rendered using visual molecular dynamics VMD software [56].

The equimolar bilayer structure which was equilibrated for ~500 ns, was taken from the earlier study [46]. The bilayer consists of 154 lipids (52 CER, 50 CHOL and 52 FFA) and 5120 water molecules with a size of 4.9 nm x 4.9 nm x 11.7 nm. The reaction coordinate of the system was chosen to be membrane normal z, where z = 0 nm corresponds to the center of mass (COM) of the lipid molecules (CER+CHOL+FFA). In our earlier work [27], diffusion coefficient (D) of drug molecules across the lipid layer was obtained and it was noted that D values changes across bilayer normal with its line averaged value found to be closer to value near the bilayer mid. Thus, in this study, for each system, molecule was kept near the mid of bilayer at ~1nm from the COM of bilayer. The system was then energy minimized and equilibrated for 10-20ns. The configuration was further simulated for 50 ns by constraining the distance between the COM of molecule and COM of bilayer. Force and position were stored at every 10 fs. Last 40 ns runs of each simulation were used to compute the transport properties of molecules through lipid layer. For each molecule, both constrained and umbrella simulations were performed to calculate diffusivity using two different techniques namely: (a) force auto-correlation function (FACF) method involving constrained simulations and (b) position auto-correlation function (PACF) method involving umbrella simulations.

For the force auto-correlation method, the diffusivity D(z) of a molecule along the bilayer normal is given by [57]

$$D(z) = \frac{(RT)^2}{\int_0^\infty < (\Delta F(z,t)\Delta F(z,0)) > dt} \quad [1]$$

$$\Delta F(z,t) = F(z,t) - < F(z,t) > \quad [2]$$

Where R is gas constant, T is temperature, F(z,t) is constrained force on molecule at a given z and <F(z,t)> is averaged force over time.

For the Position auto-correlation method, the diffusivity D(z) of molecule along the bilayer normal is given [58]

$$D(z) = \frac{(var(z))^2}{\int_0^\infty C_{zz}(t)dt} \quad [3]$$

$$C_{zz}(t) = \delta z(0) - \delta z(t) \quad [4]$$

$$\delta z(t) = z(t) - z \quad [5]$$

where var(z) is the variance of the z-component of the distance in the interval, C_{zz} is the position autocorrelation function and <z> is averaged distance over time.

2.2 Macroscopic model

Macroscopic model consists of solving governing equations with appropriate boundary conditions across skin layers namely SC (consists of lipid channels and corneocytes), VE and dermis. In order to account for finite dosage conditions an additional vehicle layer is included in the model. From the top of the vehicle, evaporation of the molecule is considered. To account for the systematic circulation in the model, sink boundary condition is applied at the bottom of the dermis. For the left and right boundaries, a periodic boundary condition (PBC) was considered, to represent a large application area.

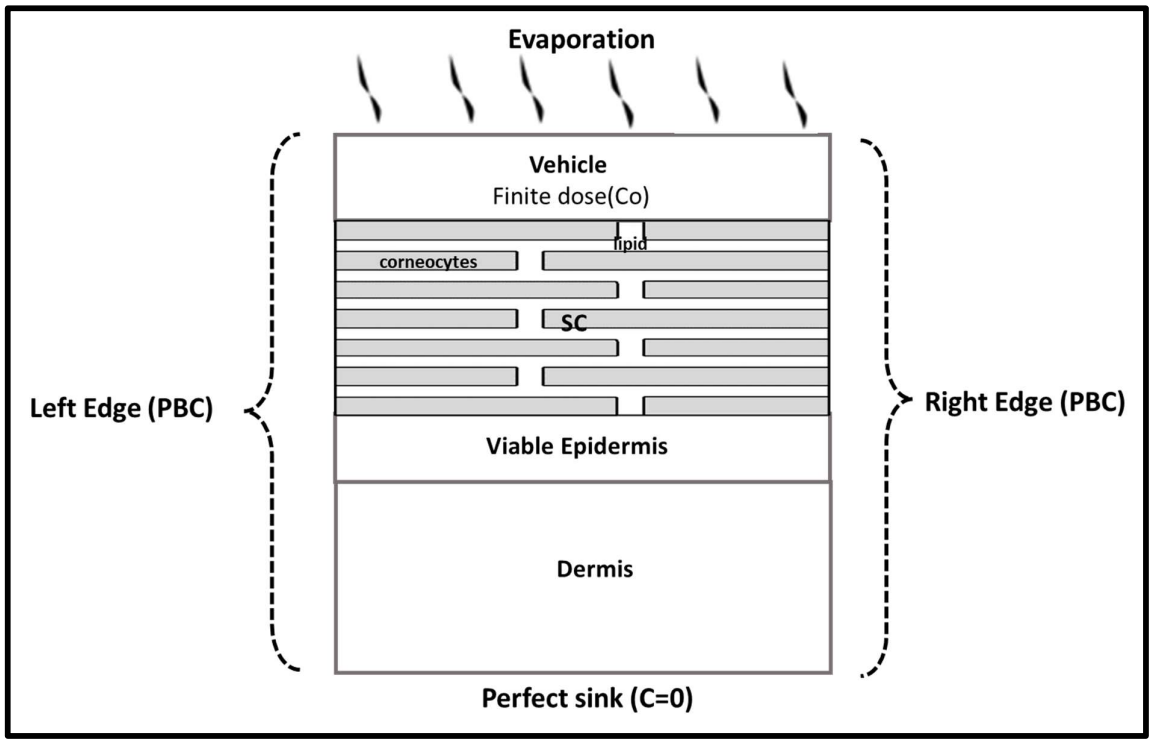

Figure 2: Geometry of skin layers considered in the simulation. figure not drawn to scale

The diffusion in the skin layers including vehicle in general is governed by Fick's 2nd law.

$$\frac{\partial C_i}{\partial t} = D_i \nabla^2 C_i \qquad [6]$$

Where, C_i = concentration of active in ith layer of skin, D_i = Diffusion coefficient of active in ith layer of Skin and t = time. i ~ v (vehicle), lip(lipid), cor(corneocytes), epi (VE), der(dermis)

and partitioning from one layer to another is given by

$$K_{i/j} = \frac{C_{i,interface}}{C_{j,interface}} \qquad [7]$$

Where $K_{i/j}$ is the partition coefficients of molecules from i^{th} layer to j^{th} layer of skin including vehicle, $C_{i,interface}$ and $C_{j,interface}$ are the concentrations at the partitioning interface of ith and jth layers.

The diffusion parameters (partition coefficient $K_{i/w}$ and diffusion coefficients D_i, for ith layer of skin including vehicle) of the different layers of the skin were either obtained from MD simulations or from empirical correlations. The Fick's 2nd law was solved for all the layers of the skin as system of PDE's

using FEM Framework with geometry of system given in Figure 2. Overall depth of skin (including SC, VE, Dermis) considered was 400±50 μm similar to that of experimental skin thickness [17]

2.2.1 Governing equations: Vehicle

The vehicle in our study was assumed to be water. A finite initial dose of molecules in the vehicle was taken from Hewitt et al. [17] . The diffusion of the molecules within vehicle was governed by the Fick's 2nd law (eq. [6]). The diffusion parameters (D_v and $K_{v/w}$) were calculated using correlations. The diffusion coefficient (D_v) of the molecule in water was calculated using the Stokes-Einstein equation [19]:

$$D_v = \frac{KT}{6\pi\eta r_s} \quad [8]$$

Where K is the Boltzmann constant, T is the temperature, η is the viscosity of water and r_s is the molecule radius (Å) calculated as [59]

$$r_s = \sqrt[3]{(3/4\pi \times 0.9087MW} \quad [9]$$

Where MW is the molecular weight of molecule.

For neutral molecules, the vehicle-water partition coefficient ($K_{v/w}$) of molecules was considered to be 1. On other hand, for ionizable molecules, the partition coefficient depends on the amount of non-ionized molecule in vehicle. Thus, the partition coefficient between vehicle and water, $K_{v/w}$ [20]

$$K_{v/w} = \frac{1}{f_{non/veh}} \quad [10]$$

Where $f_{non/veh}$ is the fraction of non-ionizable molecules in vehicle

The molecules were assumed to evaporate from the upper boundary of the vehicle. The evaporation flux is given by [28]

$$D_v \frac{\partial C_v}{\partial x} = K_{evap} \cdot \frac{\rho}{C_{v,sat}} \cdot C_v(0,t) \quad [11]$$

$$K_{evap}\rho = k_g \frac{P_{vp}MW}{0.76RT} \quad [12]$$

$$k_g = \frac{6320u^{0.78}}{MW^{1/3}} \quad [13]$$

Where K_{evap}, k_g, $C_{v,sat}$, u, P_{vp} are evaporation mass transfer coefficient, gas phase mass transfer coefficient, saturation concentration, wind velocity and molecule vapor pressure respectively. D_v and C_v are the diffusion coefficient and concentration of molecules in vehicle respectively.

On the other hand, from the bottom boundary of vehicle, the molecule diffuses into skin layers by partitioning from vehicle into the SC (lipid and corneocytes) as given by eq. [7].

2.2.2 Governing equations: SC

The SC in our study was a heterogeneous membrane comprising of lipid and corneocytes layers in brick-and-mortar fashion (Figure 2) with vehicle on top and VE at bottom.

Considering the lipid layer, to account for its tortuous path in the SC, Kushner et al. [25] came up with modified Fick's 2nd law,

$$\frac{\partial C_{lip}}{\partial t} = \left(\frac{D_{lip}}{\tau_{flux}\tau_{volume}}\right)\nabla^2 C_{lip} \qquad [14]$$

τ_{flux}, τ_{volume} = tortuosity factors to account for parallel and branched transport or active in lipid layer taken from our earlier work [27].

Modified Fick's 2nd law (eq. [14]) was used for diffusion within lipid layer and Fick's 2nd law (eq. [6]) for diffusion in the corneocytes layer. The diffusion coefficient (D_{lip}) of molecules in lipid layer was obtained from MD simulations of individual molecules in lipid bilayer and partition coefficient ($K_{lip/w}$) of molecule in lipid layer is given by [37, 60]

$$K_{lip/w} = \frac{\rho_{lip}}{\rho_w} K_{ow}^{0.69} \qquad [15]$$

Where K_{ow} is octanol-water partition coefficient respectively, ρ_{lip} and ρ_w are lipid and water bulk density respectively.

For the corneocytes layer: Partition Coefficient ($K_{cor/w}$) is given by [38]

$$K_{cor/w} = \frac{PC_{pro/w}\omega_{pro} + \upsilon}{\left(\omega_{pro}\frac{\rho_w}{\rho_{pro}}\right) + \upsilon} \qquad [16]$$

and diffusion coefficient (D_{cor}) is given by [20, 22]

$$(D_{cor})_{free} = D_w\left(1 - \varphi_f'\right)(0.9999 - 1.2762\lambda + 0.0718\lambda^2 + 0.1195\lambda^3) \qquad [17]$$

$$\left(K_{cor/w}\right)_{free} = 1 - \varphi_f' \quad [18]$$

$$K_{cor/w}D_{cor/w} = \left(K_{cor/w}\right)_{free} (D_{cor})_{free} \quad [19]$$

$$\varphi_f' = (0.1928)(1 + \lambda^2) \quad [20]$$

$$\lambda = \frac{r_s}{(35\ \text{Å})} \quad [21]$$

Where $(K_{cor/w})_{free}$ and $(D_{cor})_{free}$ are corneocytes partition and diffusion coefficient of free molecules. $PC_{pro/w}$, ω_{pro} and υ are the protein-water partition coefficient, protein mass fraction based on dry SC and water mass fraction based on dry SC. ρ_{pro} is protein water bulk density. λ represents molecule to fiber radii fraction and φ_f' is volume fraction inaccessible to the centres of molecules.

2.2.3 Governing equations: Deeper layers

The diffusion of the molecules within VE and dermis was governed by the Fick's 2nd law (eq. [6]). The partition coefficient ($K_{VE/w} \sim K_{der/w} \sim K_{epi/w}$) in the viable epidermis and dermis is assumed to be the same, and so is the diffusion coefficient (D_{epi}, m^2/s), because of the similar multiphase compositions in the two skin layers [19]

$$D_{epi} = \frac{10^{-8.15-0.655logMW}}{0.68 + \frac{0.32}{f_u} + 0.025 f_{non} K_{lip/w}} \quad [22]$$

$$K_{epi/w} = 0.7\left(0.68 + \frac{0.32}{f_u} + 0.025 f_{non} K_{lip/w}\right) \quad [23]$$

Where f_{non} and f_u are fraction of non-ionized and fraction unbound molecule.

At SC-VE interface, and VE-dermis interface, the molecules partitions from one layer to another following eq. [7].

At the bottom boundary of dermis, sink condition i.e., $C_{der}=0$ was considered. Amount of molecule permeating out of dermis was calculated as cumulative release (Q(t)) given as,

$$Q(t) = \int_0^t D_{epi}\left(\frac{\partial C_{der}\,(y,t)}{\partial y}\right)_{y=0} dt \quad [24]$$

The geometry of the skin layers along with vehicle was constructed in COMSOL Multiphysics software as shown in Figure 2. Geometric parameters (layers width, thickness, corneocyte offset etc.) were obtained from the literature [27, 17]. Geometry was meshed using triangular elements with inbuilt

meshing tool available in COMSOL software. An absolute tolerance of 10^{-6} was used in each simulation. The concentration gradient at the bottom end of the dermis was obtained from the FEM simulations. The amount of the molecules permeated through skin was calculated from the computed concentration gradient data.

A summary of diffusion parameters for FEM simulations used in present study is given in Table 1.

Table 1: Summary of physical parameters

Parameter	Description	Application layer	Value range	Reference
Dv	Diffusion Coefficient (m^2/s)	Vehicle	$8.33x10^{-10}$ to $1.18x10^{-09}$	[19]
Kv	Partition Coefficient	Vehicle	1(neutral molecules), others (based on pH)	[20]
Dlip	Diffusion Coefficient (m^2/s)	SC lipids	$2.14x10^{-10}$ to $5.95x10^{-10}$	[57]
Klip	Partition Coefficient	SC lipids	0.41-597.51	[37, 60]
Dcor	Diffusion Coefficient (m^2/s)	SC corneocytes	$2.57x10^{-11}$-$3.24x10^{-10}$	[20, 22]
Kcor	Partition Coefficient	SC corneocytes	1.85-18.95	[38]
Depi	Diffusion Coefficient (m^2/s)	Viable epidermis and Dermis	$1.32x10^{-11}$to $2.89x10^{-10}$	[19]
Kepi	Partition Coefficient	Viable epidermis and Dermis	0.79- 12.3	[19]
$\mathbf{K_{evap}\rho}$	Evaporative mass transfer coefficient (ug/cm^2hr)	Top boundary on vehicle	0.000159- 2395.08	[28]

3 Results & Discussion

In the present study, we investigated the skin permeation of 43 cosmetic-relevant chemicals taken from Ellison et al. [16] and Hewitt et al. [17]. The molecules considered varied in logKow between −0.5 and 4.76, molecular weight between 92 and 262, vapor pressure ($1.98x10^{-8}$-0.5 mmHg at 25 ◦C) and

water solubility (0.004–531 g/l), no mixtures were taken. The physical parameters were taken either from MD simulations or empirical correlations and used as input for our FEM model.

3.1 Molecular Simulation

Firstly, MD simulations for each molecule in a lipid bilayer was performed. The lipid bilayer was modeled using realistic skin lipid composition and molecule was placed inside the bilayer for simulations. The autocorrelation curve was obtained from the MD simulations and then diffusion coefficient (D_{lip}) in lipid for each molecule was calculated using two different methods FACF and PACF discussed in section 2.1 given by eq. [1] and eq. [3] respectively. A detailed explanation of calculation of D values using both methods are explained in supporting information (Figure S1-S6). The D_{lip} values from the two methods was found to be very close to each for all the molecules (supporting information Figure S7). FACF method was found to be easier to implement than PACF as PACF involves additional calculation of variance of position apart from calculation of area under the auto-correlation curves required in both the method. Considering the ease of implementation of FACF and the fact that D_{lip} values for both the methods are very close to each other, the value from FACF was considered for further study. D_{lip} for all the molecules (from FACF) with respect to their molecular weight is plotted in Figure 3. The errors in the diffusivity calculation are standard errors calculated from the difference of the diffusion coefficient in each of individual simulations at each z position from their average. D_{lip} was found to be in the range of $2x10^{-10}$ to $6x10^{-10}$ m^2/s and varying with the molecule's molecular weight. The diffusion coefficient was found to decrease with increase in the molecular weight/size of the molecule. It was noted to be of the same order and in good agreement with those obtained from experiment [16]. The D_{lip} was then used as an input in FEM simulations for the permeation study into different layers of skin. For more information on the calculation of D_{lip} please section 1 of the supporting information.

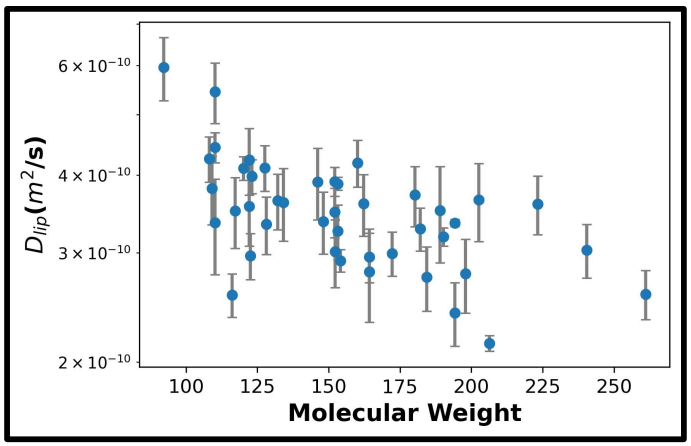

Figure 3: Diffusion coefficient of molecules in lipid bilayer obtained from MD simulation. Errors bars represent the standard error calculated from the individual diffusion coefficient for each molecule from their average diffusion coefficient plotted here.

3.2 Macroscopic model

As described in section 2, the governing equations from 3-32 were used to formulate the macroscopic model and were solved using FEM framework. For the volatile molecules involving evaporation from vehicle (eq. [[11]]), liquid-vapor equilibrium was considered at the interface of vehicle and air (ideal gas behavior was considered).

3.2.1 Simulation input and setup

The simulations were performed under finite dose conditions. The initial dose considered for all molecules in the vehicle was taken from the Hewitt et al [17]. To account for chemical volatility, the boundary condition of evaporative flux following (eq.[11]) was applied at upper boundary of the vehicle. The evaporation was considered to be a function of wind velocity at laboratory conditions (standard or fume-hood), vapor pressure of molecule and temperature. The initial concentration of molecule inside the skin layers was taken to be zero. To account for the molecule partitioning into the systematic circulation, the bottom boundary of dermis was considered to be at sink conditions. Based on the physical parameters in different layers, the molecule permeated into the skin and diffuses through the various skin layers. All the simulations were carried out for 24 hr experimental time. The total thickness of skin was considered to be around 350-450 μm, with thickness of various skin layers SC, VE and dermis were 13.05 μm, 57.57 μm and 300-375 μm respectively and vehicle thickness considered was 100 μm [18, 16, 17].The meshing of all the layers was optimized and small enough to have negligible effect on accuracy of simulations.

3.2.2 Model Results

Concentration gradient across skin layers at the bottom boundary of dermis was exported from macroscopic model. The cumulative amount of applied dose permeated through skin was calculated by numerical integration of concentration gradient data (eq. [[24]). The cumulative release profile (cumulative amount of molecule permeated through skin) as percentage of applied dose of few molecules with respect to time is plotted in Figure 4 and Figure 5. Release profiles were compared with experimental RF (receptor fluid) amount obtained from the literature [17]. The cumulative release profiles for remaining molecules can be found in supporting information 2.

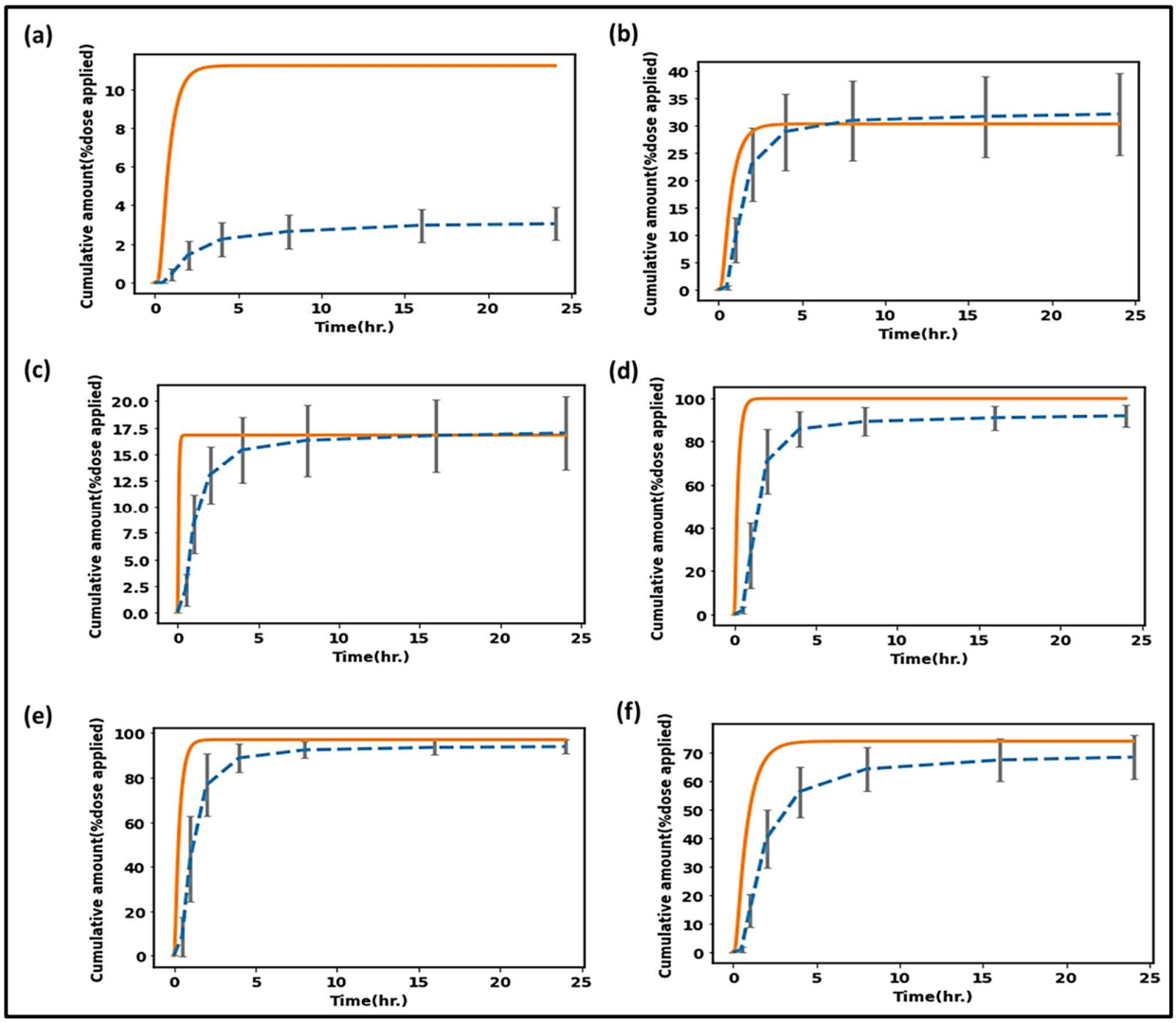

Figure 4: Percentage cumulative amount (amount in RF for experimental data) with respect to dose applied for (a) Ethylhexyl acrylate, (b) Geraniol, (c) 4-Tolunitrile, (d) 7-Ethoxycoumarin, (e) 6-Methylcoumarin, (f) Benzophenone. Experimental data(dashed line); simulation present work (solid line)

The cumulative release profiles obtained for the majority of molecules resembled a hyperbolic shape, similar to reported in literature [17]. The cumulative amount reached a plateau long before the termination of the simulation at 24 hours as shown in Figure 4. For finite doses, the observation of a plateau indicates that the molecule cannot further permeate into the skin and are attributed one or more reasons: (a) molecule evaporation due to its high volatility, (b) depletion of applied dose in vehicle due to complete permeation into skin layers (c) molecule precipitation on the surface of the skin due to solvent evaporation, (d) molecule ionization in the vehicle and skin layers (e) covalent binding related to chemical reactivity, thus preventing further permeation [18, 17]. Hewitt et al. [17] reported complete

dose depletion of molecules like 6-Methylcoumarin in the first 2-4 hrs owing to its fast diffusion resulting in hyperbolic profile, or molecule like 4-tolunitrile exhibiting hyperbolic kinetic profile due to its high volatility. Our current analysis for cumulative release also shows similar hyperbolic profile compared with the experiments. Similar results were concluded from the concentration contours in different layers for Geraniol molecule (please check section S2 of supporting information)

Figure 4a,4b,4c shows the cumulative amount obtained out of dermis is in the range 10-30% of initial dose, the loss of remaining amount could be due to above stated reasons. Binding of molecules was not accounted explicitly in our current model and the extension of ionization of these molecules the vehicle is negligible, owing to their partition coefficient $K_{v/w}$ to be very close to one. So, Ethylhexyl acrylate, Geraniol and 4-Tolunitrile as shown in Figure 4a,4b,4c respectively were found to be highly volatile and have mostly evaporated from vehicle instead of diffusing into the vehicle. This was further confirmed by comparing the mass balance calculations across skin layers. Around 70-90 % of initial dose of Ethylhexyl acrylate, Geraniol and 4-Tolunitrile evaporated from the vehicle (Figure 6, see supporting information 2 for more information on mass balance amounts). On the other hand, 7-Ethoxycoumarin, 6-Methylcoumarin and Benzophenone were found to almost diffuse completely in the first few hours as shown in Figure 4d,4e,4f respectively. For molecules like these, the rate of diffusion was very fast as compared to their evaporation rate, which allowed most of the amount to diffuse out the dermis.

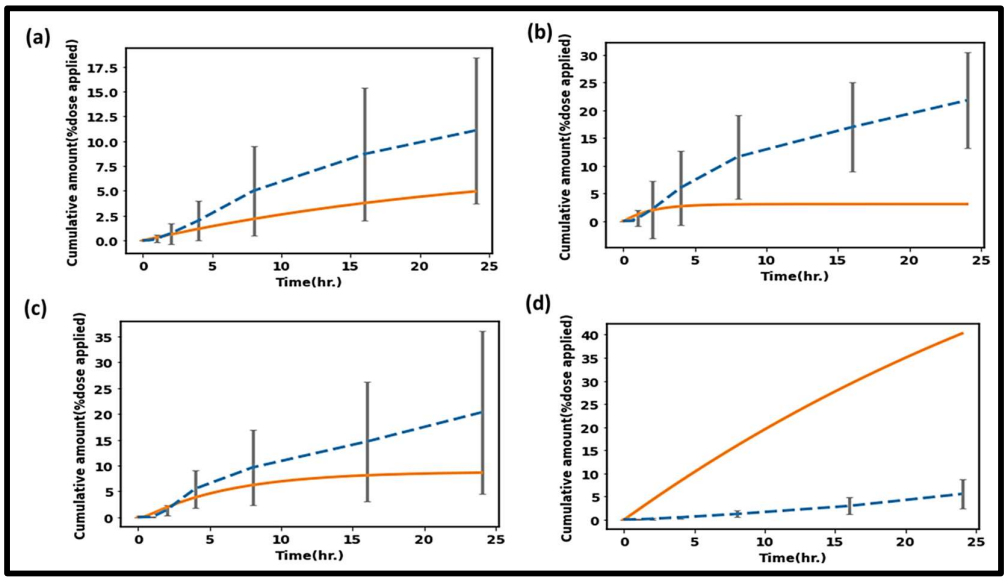

Figure 5: Percentage cumulative amount (amount in RF for experimental data) with respect to dose applied for (a) Thioglycolic acid (b) Cinnamic acid (c) Ibuprofen (d) 4-Chlorobutyric acid. Experimental data(dashed line); simulation present work (solid line)

Apart from these molecules, there were few other cases in which the cumulative amounts do not follow a hyperbolic profile to reach plateau. As shown in Figure 5, these molecules presented a slow and near linear cumulative release profile. This could be attributed to multiple reasons such as (a) Ionization of molecules in the vehicle itself leading to very less amount of non-ionized molecule to permeate inside (b) slow diffusion kinetics through the skin layers (c) faster evaporation rates from vehicle.

Ionization of the molecules in the vehicle was found to have significant effect on the molecule's vehicle-water partition coefficient and was the main factor responsible for their near linear profile as noted from the cumulative profile shown in Figure 5. For Thioglycolic acid ($K_{v/w}$ =5012.9), Cinnamic acid ($K_{v/w}$ =1149.15), Ibuprofen ($K_{v/w}$ =933), and 4-Chlorobutyric acid ($K_{v/w}$ =795.33), their $K_{v/w}$ were found to be much higher as compared to neutral non-ionizing molecule ($K_{v/w}$ ~1), since all four of them are acidic in nature with pKa value of 3.7, 4.34, 4.4 and 4.5 respectively, which led to their ionization in vehicle itself and resulted in very less amount of non-ionized molecule permeating inside.

A difference between the permeation data obtained from experimental and simulation data was noted as shown in Figure 5, which could be attributed to a variety of reasons (a) non consideration of pH effect in SC (b) non consideration of explicit binding of molecules within skin layers (c) non consideration of precipitation of molecules on surface of skin. Apart from these reasons, the vehicle solvent taken in present study was water whereas in experiments [17], PBS (phosphate buffered saline) was used. This could affect the diffusion parameter of vehicle. Hewitt et al. [17], reported molecules like Thioglycolic acid, Cinnamic acid, Ibuprofen and 4-Chlorobutyric acid having high amounts of these obtained in skin wash (amount remaining on surface of skin due to precipitation or staying in the vehicle due to ionization) in the range 55-85 % of applied dose, which was not accounted for in current model.

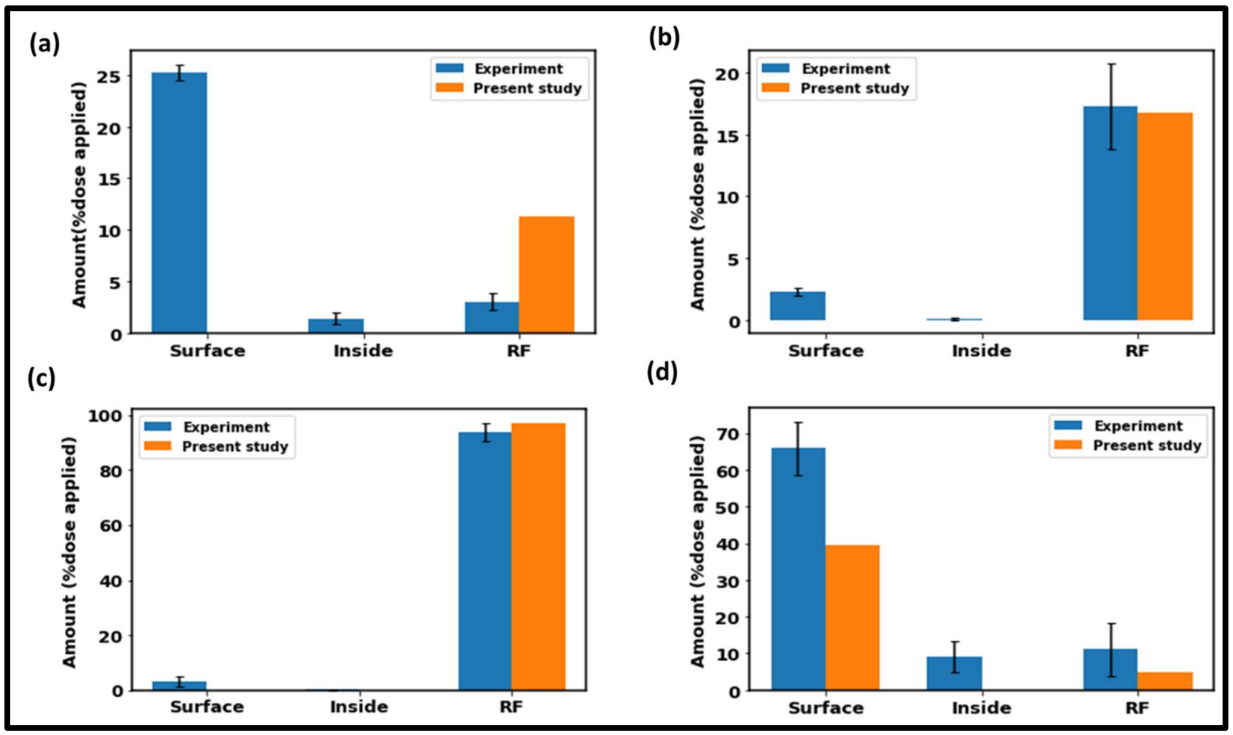

Figure 6: Percentage amount distribution (with respect to dose applied) comparison between experiments [17] and present study at the end of 24hrs. for (a) Ethylhexyl acrylate, (b) 4-Tolunitrile, (c) 6-Methylcoumarin (d) Thioglycolic acid in different layers: Surface(amount left in vehicle or precipitated on surface), Inside(Total amount present in SC,VE and Dermis) and RF (Total amount released out of dermis). Experimental data(Blue); simulation present work (orange).

A study of mass balance of the total amount distribution further provided a clear reason for discrepancy between experimental and simulation results. To further investigate the discrepancy between experiments and simulation results, a mass balance calculation across skin layers was made. For this, a comparative analysis of the amount distribution of molecule in the different skin layers and vehicle for the experimental and simulations setup was performed at the end of computation time (i.e. after 24hrs). The analyzed data has been plotted in Figure 6. For this, the data was divided in three layers (i) Surface: total amount left in the vehicle or on the surface (ii) Inside: total amount accumulated inside SC, VE and dermis (iii) RF: total amount released out of dermis. The amount missing from total mass balance was the evaporated molecule amount from the vehicle. The RF amount in present study was found to be comparable to that of experimental results but, a significant difference was found in the Surface amount as shown in Figure 6. This could be due to a number of reasons, an important one being, precipitation of molecules on surface of skin were not accounted for in our study. The molecule could precipitate on the skin surface once the solution evaporated and therefore, the rate-limiting step

may be related more to the dissolution rate of precipitated molecule rather than the diffusion through the SC [18, 17]. Our model doesn't account for this dynamic behavior leading to the deviation compared with the experiments. The accumulated amount inside the skin layers (shown in Figure 6) compared with experimental data do not have good agreement. Poor prediction of amount distribution from the model despite good agreement between RF could be due to, the model had captured the key mechanisms that impact RF amount, or the combination empirical relations used in our model gives good RF prediction, but the specific chemical factors affecting amount distribution have not been accounted for.

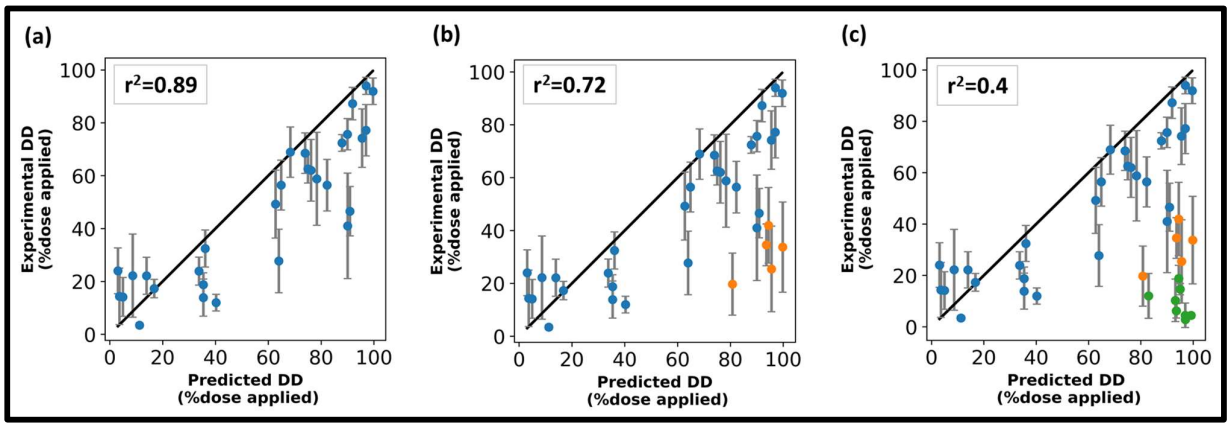

Figure 7: Comparative analysis of dermal delivery(DD) after 24 hr. experiment time. (a) 30 molecules, r^2~0.89 (molecules plotted in blue) (b) 35 molecules, r^2~0.72 (the additional molecules from (a) are plotted in orange), (c) 43 molecules r^2~0.4 (the additional molecules from (b) are plotted in green)

For analyzing overall effectiveness and accuracy of the model, a comparison between experimental DD [17] and predicted DD was performed from the data plotted in Figure 7 (DD is total amount present in VE, dermis and RF). For 30 molecules having good, r^2 ~ 0.89 was calculated (molecules shown in blue in Figure 7(a)), which decreased to r^2 ~0.72 for 35 molecules (additional molecules shown in orange in Figure 7(b)) and further for 43 molecules r^2 ~0.4 (additional molecules shown in green in Figure 7(c)). This sharp decrease in r^2 was noted to be due to bad correlation for few molecules (mainly Methyl Methane sulfonate, 2-Acetyl amino fluorene, Tetramethyl thiuram disulfide, HC Red No.3, 2,5-Diaminotoluene sulfate). These molecules have error percentage of around 90% between experimental and simulation data. Further examining the experimental and simulations data, it was noted that these outliers have around 70-80% of applied dose obtained in skin wash after the end of 24 hr. experiments [17], which has not been accounted for in our model resulting in huge discrepancy in experimental and simulation results (please see supporting information 2 for more details).

Overall, for most molecules a good correlation between simulation and experimental results was obtained. There are few outliers, with significant difference which requires further improvement of the model. This discrepancy could be due a number of reasons discussed before. Among important ones were, in our model, lack of molecular binding in some of the layers of the skin, molecule precipitation on the surface of the skin due to solvent evaporation was not accounted for, ionization of molecules in the SC was not considered. Thickness of skin layers could also be another source of discrepancy. Future experimental and simulation studies will be needed to investigate which parameters are important in determining the local concentrations of molecules in the skin as well as to identify binding of molecules in respective layers.

4 Conclusions

In this study, we have extended integrated multiscale model (MD and FEM) of skin SC layer to deeper skin layer with finite dose condition. Several constrained MD simulations were performed to calculate the diffusion coefficient of the molecules in the lipid layers and the physical parameters were used in the FEM for permeation study of 43 cosmetic relevant molecules. Considering a realistic exposure scenario, i.e. a finite amount of various molecules applied on skin, the main outcome of this study highlighted the importance of chemical volatility and ionization of molecules (i.e. pH) which improved model predictions for few molecules. The obtained release profile of different molecules using macroscopic model shows good qualitative agreement with experiments.

It is important to note that integrated multi-scale model (molecular and macroscopic models) presented here does show a good qualitative match between experiments and simulations. However, there are certain limitations which need to be overcome to make it more robust. Inclusion of molecule precipitation on the surface of skin and binding within skin layers could further improve our model. Our model has mostly used diffusion parameters obtained from empirical relations found in literature and is not dependent experimentally derived coefficients.

Acknowledgement

Authors would like to thank Dr Naga Neehar Dingari for his suggestions on FEM modeling, Dr Gautam Shroff, Head, TCS Research and Mr. K Ananth Krishnan, CTO and EVP, Tata Consultancy Services for their constant encouragement and support during this project.

Funding & Resources

This research was funded by Tata Consultancy Services (TCS), CTO organization.

Conflict of interest

The authors declare no conflicts of interest.

References

[1] A. Zaid Alkilani, M. T. McCrudden and R. F. Donnelly, "Transdermal drug delivery: innovative pharmaceutical developments based on disruption of the barrier properties of the stratum corneum," *Pharmaceutics,* vol. 7, pp. 438-470, 2015.

[2] R. L. Gallo, "Human skin is the largest epithelial surface for interaction with microbes," *Journal of Investigative Dermatology,* vol. 137, pp. 1213-1214, 2017.

[3] X. Liu, P. Kruger, H. Maibach, P. B. Colditz and M. S. Roberts, "Using skin for drug delivery and diagnosis in the critically ill," *Advanced drug delivery reviews,* vol. 77, pp. 40-49, 2014.

[4] G. K. Menon, "New insights into skin structure: scratching the surface," *Advanced drug delivery reviews,* vol. 54, pp. S3-S17, 2002.

[5] C. M. Schoellhammer, D. Blankschtein and R. Langer, "Skin permeabilization for transdermal drug delivery: recent advances and future prospects," *Expert opinion on drug delivery,* vol. 11, pp. 393-407, 2014.

[6] T. Gratieri, I. Alberti, M. Lapteva and Y. N. Kalia, "Next generation intra-and transdermal therapeutic systems: using non-and minimally-invasive technologies to increase drug delivery into and across the skin," *European Journal of Pharmaceutical Sciences,* vol. 50, pp. 609-622, 2013.

[7] Y. Gilaberte, L. Prieto-Torres, I. Pastushenko and Á. Juarranz, "Anatomy and Function of the Skin," in *Nanoscience in Dermatology*, Elsevier, 2016, pp. 1-14.

[8] J. Kanitakis, "Anatomy, histology and immunohistochemistry of normal human skin," *European journal of dermatology,* vol. 4, no. 12, pp. 390-401, 2002.

[9] A. Joshi and J. Raje, “Sonicated transdermal drug transport,” *Journal of controlled release,* vol. 83, pp. 13-22, 2002.

[10] S. Cross and M. Roberts, “Physical enhancement of transdermal drug application: is delivery technology keeping up with pharmaceutical development?,” *Current drug delivery,* vol. 1, pp. 81-92, 2004.

[11] N. Dragicevic and H. I. Maibach, Percutaneous penetration enhancers physical methods in penetration enhancement, New York, NY, USA: Springer, 2017.

[12] J. A. Subramony, “Needle free parenteral drug delivery: Leveraging active transdermal technologies for pediatric use,” *International journal of pharmaceutics,* vol. 455, pp. 14-18, 2013.

[13] V. Dhote, P. Bhatnagar, P. K. Mishra, S. C. Mahajan and D. K. Mishra, “Iontophoresis: a potential emergence of a transdermal drug delivery system,” *Scientia pharmaceutica,* vol. 80, pp. 1-28, 2012.

[14] R. J. Silva and S. Tamburic, “A State-of-the-Art Review on the Alternatives to Animal Testing for the Safety Assessment of Cosmetics,” *Cosmetics,* vol. 9, no. 5, p. 90, 2022.

[15] S. Adler, D. Basketter, S. Creton, O. Pelkonen, J. Van Benthem, V. Zuang, K. E. Andersen, A. Angers-Loustau, A. Aptula and A. Bal-Price , “Alternative (non-animal) methods for cosmetics testing: current status and future prospects—2010,” *Archives of toxicology,* vol. 85, no. 5, pp. 367-485, 2011.

[16] C. A. Ellison, K. O. Tankersley, C. M. Obringer, G. J. Carr, J. Manwaring, H. Rothe, H. Duplan, C. Géniès, S. Grégoire and N. J. Hewitt, “Partition coefficient and diffusion coefficient determinations of 50 compounds in human intact skin, isolated skin layers and isolated stratum corneum lipids,” *Toxicology in Vitro,* vol. 69, no. 104990, pp. 0887-2333, 2020.

[17] N. J. Hewitt, S. Grégoire, R. Cubberley, H. Duplan, J. Eilstein, C. Ellison, C. Lester, E. Fabian, J. Fernandez and C. Géniès, “Measurement of the penetration of 56 cosmetic relevant chemicals into and through human skin using a standardized protocol,” *Journal of Applied Toxicology,* vol. 40, pp. 403-415, 2020.

[18] S. Grégoire, I. Sorrell, D. Lange, A. Najjar, A. Schepky, C. Ellison, J. Troutman, E. Fabian, H. Duplan and C. Genies, "Cosmetics Europe evaluation of 6 in silico skin penetration models," *Computational Toxicology,* vol. 19, p. 100177, 2021.

[19] T. Chen, G. Lian and P. Kattou, "In silico modelling of transdermal and systemic kinetics of topically applied solutes: model development and initial validation for transdermal nicotine," *Pharmaceutical Research,* vol. 33, pp. 1602-1614, 2016.

[20] Y. Dancik, M. A. Miller, J. Jaworska and G. B. Kasting, "Design and performance of a spreadsheet-based model for estimating bioavailability of chemicals from dermal exposure," *Advanced drug delivery reviews,* vol. 65, no. 2, pp. 221-236, 2013.

[21] M. A. Miller and G. B. Kasting, "A spreadsheet-based method for simultaneously estimating the disposition of multiple ingredients applied to skin," *Journal of Pharmaceutical Sciences,* vol. 104, no. 6, pp. 2047-2055, 2015.

[22] T. Wang, G. B. Kasting and J. M. Nitsche, "A multiphase microscopic diffusion model for stratum corneum permeability. II. Estimation of physicochemical parameters, and application to a large permeability database," *Journal of pharmaceutical sciences,* vol. 96, no. 11, pp. 3024-3051, 2007.

[23] J. E. Rim, P. M. Pinsky and W. W. van Osdol, "Finite element modeling of coupled diffusion with partitioning in transdermal drug delivery," *Annals of biomedical engineering,* vol. 33, pp. 1422-1438, 2005.

[24] J. E. Rim, P. M. Pinsky and W. W. van Osdol, "Multiscale modeling framework of transdermal drug delivery," *Annals of biomedical engineering,* vol. 37, pp. 1217-1229, 2009.

[25] J. Kushner IV, W. Deen, D. Blankschtein and R. Langer, "First-principles, structure-based transdermal transport model to evaluate lipid partition and diffusion coefficients of hydrophobic permeants solely from stratum corneum permeation experiments," *Journal of pharmaceutical sciences,* vol. 96, pp. 3236-3251, 2007.

[26] H. F. Frasch and A. M. Barbero, "Steady-state flux and lag time in the stratum corneum lipid pathway: Results from finite element models," *Journal of Pharmaceutical Sciences,* vol. 92, pp. 2196-2207, 2003.

[27] K. Gajula, R. Gupta, D. Sridhar and B. Rai, "In-Silico skin model: a multiscale simulation study of drug transport," *Journal of chemical information and modeling,* vol. 57, no. 8, pp. 2027-2034, 2017.

[28] G. B. Kasting and M. A. Miller, "Kinetics of finite dose absorption through skin 2: volatile compounds," *Journal of pharmaceutical sciences,* vol. 95, no. 2, pp. 268-280, 2006.

[29] N. A. Monteiro-Riviere, Toxicology of the Skin, CRC Press, 2010.

[30] L. Franzen and M. Windbergs, "Applications of Raman spectroscopy in skin research—from skin physiology and diagnosis up to risk assessment and dermal drug delivery," *Advanced drug delivery reviews,* vol. 89, pp. 91-104, 2015.

[31] W. Montagna, The structure and function of skin, Elsevier, 2012.

[32] I. Iwai, H. Han, L. Den Hollander, S. Svensson, L.-G. Öfverstedt, J. Anwar, J. Brewer, M. Bloksgaard, A. Laloeuf and D. Nosek, "The human skin barrier is organized as stacked bilayers of fully extended ceramides with cholesterol molecules associated with the ceramide sphingoid moiety," *Journal of Investigative Dermatology,* vol. 132, no. 9, pp. 2215-2225, 2012.

[33] J. M. Nitsche and H. F. Frasch, "Dynamics of diffusion with reversible binding in microscopically heterogeneous membranes: General theory and applications to dermal penetration," *Chemical engineering science,* vol. 66, no. 10, pp. 2019-2041, 2011.

[34] E. Abd, S. A. Yousef, M. N. Pastore , K. Telaprolu, Y. H. Mohammed, S. Namjoshi, J. E. Grice and M. S. Roberts, "Skin models for the testing of transdermal drugs," *Clinical pharmacology: advances and applications,* vol. 8, p. 163, 2016.

[35] F. Pirot, Y. N. Kalia, A. L. Stinchcomb, G. Keating, A. Bunge and R. H. Guy, "Characterization of the permeability barrier of human skin in vivo," *Proceedings of the National Academy of Sciences,* vol. 94, pp. 1562-1567, 1997.

[36] A. L. M. Ruela, A. G. Perissinato, M. E. d. S. Lino, P. S. Mudrik and G. R. Pereira, "Evaluation of skin absorption of drugs from topical and transdermal formulations," *Brazilian Journal of Pharmaceutical Sciences,* vol. 52, pp. 527-544, 2016.

[37] S. Mitragotri, "Modeling skin permeability to hydrophilic and hydrophobic solutes based on four permeation pathways," *Journal of Controlled Release,* vol. 86, no. 1, pp. 69-92, 2003.

[38] J. M. Nitsche, T.-F. Wang and G. B. Kasting, "A two-phase analysis of solute partitioning into the stratum corneum," *Journal of pharmaceutical sciences,* vol. 95, no. 3, pp. 649-666, 2006.

[39] L. Norlén, B. Forslind, I. Nicander, B. L. Rozell and S. Ollmar, "Inter-and intra-individual differences in human stratum corneum lipid content related to physical parameters of skin barrier function in vivo," *Journal of investigative dermatology,* vol. 112, pp. 72-77, 1999.

[40] A. Weerheim and M. Ponec, "Determination of stratum corneum lipid profile by tape stripping in combination with high-performance thin-layer chromatography," *Archives of dermatological research,* vol. 293, pp. 191-199, 2001.

[41] E. Mojumdar, Z. Kariman, L. Van Kerckhove, G. Gooris and J. Bouwstra, "The role of ceramide chain length distribution on the barrier properties of the skin lipid membranes," *Biochimica et Biophysica Acta (BBA)-Biomembranes,* vol. 1838, pp. 2473-2483, 2014.

[42] R. Gupta, D. Sridhar and B. Rai, "Molecular dynamics simulation study of permeation of molecules through skin lipid bilayer," *The Journal of Physical Chemistry B,* vol. 120, no. 34, pp. 8987-8996, 2016.

[43] O. Berger , O. Edholm and F. Jähnig, "Molecular dynamics simulations of a fluid bilayer of dipalmitoylphosphatidylcholine at full hydration, constant pressure, and constant temperature," *Biophysical journal,* vol. 72, no. 5, pp. 2002-2013, 1997.

[44] C. Das, M. G. Noro and P. D. Olmsted, "Lamellar and inverse micellar structures of skin lipids: effect of templating," *Physical review letters,* vol. 111, no. 14, p. 148101, 2013.

[45] R. Notman, W. K. den Otter, M. G. Noro, W. J. Briels and J. Anwar, "The permeability enhancing mechanism of DMSO in ceramide bilayers simulated by molecular dynamics," *Biophysical journal,* vol. 93, no. 6, pp. 2056-2068, 2007.

[46] R. Gupta and B. Rai, "Molecular dynamics simulation study of skin lipids: effects of the molar ratio of individual components over a wide temperature range," *The Journal of Physical Chemistry B,* vol. 119, no. 35, pp. 11643-11655, 2015.

[47] M. Höltje, T. Förster, B. Brandt, T. Engels, W. von Rybinski and H.-D. Höltje, "Molecular dynamics simulations of stratum corneum lipid models: fatty acids and cholesterol," *Biochimica et Biophysica Acta (BBA)-Biomembranes,* vol. 1511, no. 1, pp. 156-167, 2001.

[48] N. Schmid, A. P. Eichenberger, A. Choutko, S. Riniker, M. Winger, A. E. Mark, and W. F. van Gunsteren , "Definition and testing of the GROMOS force-field versions 54A7 and 54B7," *European biophysics journal,* vol. 40, no. 7, pp. 843-856, 2011.

[49] H. Berendsen, J. Postma, W. F. van Gunsteren and J. Hermans , "Interaction Models for Water in Relation to Protein Hydration," in *Intermolecular Forces: Proceedings of the Fourteenth Jerusalem Symposium on Quantum Chemistry and Biochemistry Held in Jerusalem, Israel, April 13–16, 1981*, Springer Netherlands, 1981, pp. 331-342.

[50] B. Hess, C. Kutzner, D. Van Der Spoel and E. Lindahl, "GROMACS 4: algorithms for highly efficient, load-balanced, and scalable molecular simulation," *Journal of chemical theory and computation,* vol. 4, no. 3, pp. 435-447, 2008.

[51] D. Van Der Spoel, E. Lindahl, B. Hess, G. Groenhof, A. E. Mark and H. J. Berendsen, "GROMACS: fast, flexible, and free," *Journal of computational chemistry,* vol. 26, no. 16, pp. 1701-1718, 2005.

[52] H. J. Berendsen, D. van der Spoel and R. van Drunen, "GROMACS: A message-passing parallel molecular dynamics implementation," *Computer physics communications,* vol. 91, no. 1-3, pp. 43-56, 1995.

[53] S. Pronk, S. Páll, R. Schulz, P. Larsson, P. Bjelkmar, R. Apostolov, M. R. Shirts, J. C. Smith, P. M. Kasson and D. Van Der Spoel, "GROMACS 4.5: a high-throughput and highly parallel open source molecular simulation toolkit," *Bioinformatics,* vol. 29, no. 7, pp. 845-854, 2013.

[54] M. J. Abraham, T. Murtola, R. Schulz, S. Páll, J. C. Smith, B. Hess and E. Lindahl, "GROMACS: High performance molecular simulations through multi-level parallelism from laptops to supercomputers," *SoftwareX,* vol. 1, pp. 19-25, 2015.

[55] B. Hess, H. Bekker, H. J. Berendsen and J. G. Fraaije, "LINCS: a linear constraint solver for molecular simulations," *Journal of computational chemistry,* vol. 18, no. 12, pp. 1463-1472, 1997.

[56] W. Humphrey, A. Dalke and K. Schulten, “VMD: visual molecular dynamics,” *Journal of molecular graphics,* vol. 14, no. 1, pp. 33-38, 1996.

[57] S.-J. Marrink and H. J. Berendsen, “Simulation of water transport through a lipid membrane,” *The Journal of Physical Chemistry,* vol. 98, no. 15, pp. 4155-4168, 1994.

[58] T. Casalini, A. Rosolen, C. Y. H. Henriques and G. Perale , “Permeation of biopolymers across the cell membrane: a computational comparative study on polylactic acid and polyhydroxyalkanoate,” *Frontiers in bioengineering and biotechnology,* vol. 8, p. 718, 2020.

[59] S. Mitragotri, M. E. Johnson, D. Blankschtein and R. Langer, “An analysis of the size selectivity of solute partitioning, diffusion, and permeation across lipid bilayers,” *Biophysical journal,* vol. 77, no. 3, pp. 1268-1283, 1999.

[60] L. Chen, G. Lian and L. Han, “Use of “bricks and mortar” model to predict transdermal permeation: model development and initial validation,” *Industrial & engineering chemistry research,* vol. 47, no. 17, pp. 6465-6472, 2008.